Macromolecules
ARTICLE

Macromolecules **2010**, *43*, 2933–2941 **2933**
DOI: 10.1021/ma9027933

Effect of Particles on the Flow-Induced Crystallization of Polypropylene at Processing Speeds

Michelle D'Haese,[†] Peter Van Puyvelde,*[,†] and Florentin Langouche[‡]

[†]*Department of Chemical Engineering, Leuven Materials Research Centre MRC, Katholieke Universiteit Leuven, W. De Croylaan 46, 3001 Leuven, Belgium, and* [‡]*Solvay Central Laboratory, Neder Over Heembeek, Rue de Ransbeek 310, 1120 Brussels, Belgium*

Received December 18, 2009; Revised Manuscript Received February 8, 2010

ABSTRACT: The effect of particles with different diameters on flow-induced crystallization from low shear rates to processing speeds is studied using mixtures of polypropylene and zinc oxide with diameters between 35 nm and 1 μm. The nucleating efficiency of the particles was characterized by means of the Lotz efficiency scale using DSC. Flow-induced crystallization at processing speeds was studied by means of the birefringence and transmitted intensity measurements using a specially designed sliding-plate flow cell. For crystallization under quiescent conditions and after shear steps at low shear rates, there are significant differences between the kinetics of the neat polymer, the mixture with the 1 μm zinc oxide, and the mixtures with the midrange particles, which are in agreement with the nucleating efficiency of the particles. As the shear rate is increased, the crystallization kinetics of the mixtures and neat polymer become similar, independent of particle diameter. The transition to highly oriented shish-kebab structures occurs somewhat earlier as the nucleating efficiency is higher, but at the highest shear rates, the kinetics of all materials are equal. This suggests a gradual shift in dominance from the influence of particle addition on the crystallization process at low speeds to the influence of flow at high speeds.

1. Introduction

Many of the plastic products used in everyday life are in the semicrystalline solid state. During processing, the polymers are subjected to complex and often intense flow fields which will influence the subsequent crystallization and hence the morphology and properties of a product.[1,2]

The effect of thermomechanical history on polymer crystallization has been studied extensively in the past decades (e.g., reviews[3−5]). It is now well established that flow mainly affects the nucleation step in polymer crystallization, leading to an acceleration of the crystallization process.[3,6−10] As for morphology, sufficiently intense flow might cause a structural transition from isotropic spherulitic to highly oriented "shish-kebab" structures.[3,11−13] A detailed picture of the formation of these highly anisotropic shish-kebab structures is slowly emerging in the literature.[3,7,14−19]

In case of shear flow, studies have often been conducted under well-controlled rheometric flow conditions, such as simple shear flow. The drawback of this approach is that only relatively low shear rate values can be achieved due to instrument limitations.[8−10,20] In many of these studies, continuous flow was applied throughout crystallization,[10,21,22] causing the flow to interfere with the growing crystallites. In order to overcome this problem, Janeschitz-Kriegl et al.[6] pioneered the so-called "short time shearing protocol" in which the shearing time is taken short enough to avoid interference of the flow with the crystal growth, which allows separating the nucleation and growth phenomena. This protocol - still limited to moderate shear conditions - has proven to be successful in the study of flow-induced crystallization, for instance in rheometry experiments[20,23,24] and in experiments with modified rotational shear cells in which a rheometric flow is combined with optical measurements.[25,26]

*To whom correspondence should be addressed. E-mail: Peter.Vanpuyvelde@cit.kuleuven.be.

In order to reach the processing shear rate range, another approach has been followed by various researchers, often in combination with the Janeschitz-Kriegl protocol.[1,2,6,27] These studies concerned extrusion- or injection-molding-like setups, which have the undeniable advantage of being able to approach industrial reality, but which, on the other hand, generate a nonhomogeneous flow field with a large distribution of shear rates throughout the sample, leading to the typical skin-core morphologies.

Recently, the gap between rheometrically well-controlled and complex processing-like flows was bridged by Langouche[28] and by Baert et al.[29] These authors used a sandwich-type sliding plate shear cell with optical access, able to impose homogeneous shear flow at shear rates and strains well into the processing regime.

It has to be remarked that most of the studies on flow-induced crystallization have been carried out on relatively pure polymers. However, in reality, polymers always contain an additive package, added for a variety of reasons. The influence of additives and in particular particles, the category considered in this study, on the quiescent crystallization of polymers has been the subject of many studies.[30−37] In view of the large variety in polymer−particle combinations, a complete literature review concerning this subject is beyond the scope of this paper. However, in general, it can be stated that the effect of particle addition on crystallization is determined by the particle characteristics (such as concentration, composition, particle size, and shape) and by the interactions between the particle and the polymer.[31−33] Many particles ("nucleating agents") have been found to increase heterogeneous nucleation in semicrystalline polymers, thereby accelerating the crystallization process.[30,31,34−36] As for the effect of particles on crystal growth rate, it is sometimes suggested that occlusion or rejection of particles may disturb crystal growth,[38] though this is generally not a very strong effect.

The combined effect of shear flow and particles on the crystallization of polymers has not yet been studied systematically in the

Published on Web 02/26/2010

literature, though it is clear that a profound influence on both structure formation and properties of products can be expected.[1,2] Some studies have been carried out at a single shear rate/strain combination,[39−41] often high enough to induce strongly oriented morphologies but unable to provide a systematic view of the separate contributions of flow and particles to the crystallization process. In other studies, a more elaborate range of shear rates has been investigated, but these are often limited to low or moderate shear conditions.[42−45] A third type of studies concerns experiments involving complex flow histories (e.g., duct flow[46] or fiber drawing experiments[47,48]), in which the shear conditions are similar to those encountered in industrial processing. The main difficulty in these experiments, though, is to discern between the influences of different parameters.

Both particles and shear flow influence nucleation density, which in turn determines the kinetics of the crystallization process. Hence, the contribution of both relative to each other is expected to be of importance.[9] In studies concerning a range of (moderate) shear conditions, it has often been reported that the acceleration of the crystallization kinetics with increasing shear rate is less drastic for polymers containing a nucleating agent.[42−44,46−48]

In an early study by Lagasse and Maxwell[42] and also in a more recent work by Naudy et al.[44] for low to moderate shear rates, this observation was explained as due to an additive effect. Under quiescent conditions, a nucleating agent will increase the nucleation density of a polymer; applying shear also enhances nucleation. The increase in nucleation density caused by moderate shear flow, however, will be relatively less important for the polymer with nucleating agent, since it already has a higher nucleation density under quiescent conditions. Therefore, these authors considered the contributions of nucleating agent and shear flow to nucleation density to be additive: at low shear rates the contribution of the particles dominates; at higher shear rates the contribution of flow becomes more important.

In other studies, the relative contribution of flow and particles to the crystallization process was considered in a different way, namely as resulting from a specific interaction or synergy between the particles and the surrounding polymer matrix. For instance, Janeschitz-Kriegl's group[46] proposed a nucleation mechanism in which particles serve as point nuclei on which polymer chains can absorb and subsequently stretch in the flow field to form thread-like precursors. This theory was used to explain why in nucleated samples crystallized after duct flow orientation was enhanced as compared to neat samples. This observation of enhanced orientation has been made in practically all studies concerning the influence of (intense) flow on nucleated polymers.[1,39,40,43,45−48]

Building on the point-nucleation theory in Jerschow et al.,[46] or proposing it as an independent hypothesis, many authors have explained the synergy between particles and matrix as originating from changes in the local stress levels and orientation of the polymer chains surrounding a particle.[39,43,45] These studies often involved intercalated nanoclay particles, for which the contact area between polymer and particle surface is very large. Simulations by Hwang et al.[49] supported the notion that local stress variations would lead to increased orientation and indicated the existence of a critical interparticle distance for this interaction.

Making the assumption of a synergetic effect between particles and polymer does not rule out that the effect of shear may also be dependent on the quiescent nucleation density. Byelov et al.[41] identified both nucleation by the particles, by the flow, and by the interaction between these two as competing contributions to the total number of nuclei, supporting this with estimations of each contribution. The same reasoning, but in somewhat less detail, was followed by Kelarakis et al.[40]

This study aims to bridge the gap between single-point, moderate-shear-range, and complex-flow studies conducted until now by studying the behavior of particle-filled materials after applying simple shear flow from low shear rates up to processing rates at constant strain. As it might be expected that particles with dimensions similar to those of the polymer chains will interact differently with their matrix than micrometer scaled ones, the particle dimensions have been varied from nano- to micrometer scale.

Table 1. Specific Surface of the Different Zinc Oxides

av diameter particles	35 nm	200 nm	500 nm	1 μm
specific surface [m^2/g]	30	8	4.5	1.6

2. Experimental Section

Materials. An isotactic polypropylene obtained from Borealis GMBH was used in this study. Material properties and a rheological characterization can be found in the Supporting Information.

Zinc oxide particles with average diameters of 35 nm, 200 nm, 500 nm, and 1 μm, obtained from Umicore Group Zinc Chemicals, have been chosen as filler material. Whereas the 35 nm particles are rather oblong, the 200 and 500 nm particles are relatively spherical and the 1 μm particles are irregular in shape, containing separate and clustered rodlike and spikelike particles (images can be found in the Supporting Information). Despite the differences in shape, the specific surface of the particles, as determined by gas adsorption by the producer (Table 1), still correlates with the particle diameter.

Mixtures of the polypropylene with 1 wt % (~0.16 vol %) of each zinc oxide were made by means of a twin-screw mini-extruder (DSM-Research, The Netherlands). The mini-extruder consists of a mixing chamber with a capacity of 15 mL and two corotating conical screws. A recirculation channel within the mixing chamber allows variation of the residence time. The screw speed was set at 100 rpm, and the material was allowed to recirculate for 5 min at 220 °C. To avoid degradation N_2 was circulated through the extruder during mixing. It was verified by means of scanning electron microscopy that a reasonably good dispersion of the particles was obtained in all cases.

Methods. DSC experiments have been performed with a DSC Q2000 (Universal V4.3A TA Instruments) to determine the quiescent crystallization kinetics of the mixtures and the nucleating efficiency of the particles. Samples of 5−10 mg were cut from the polymer pellets.

The flow-induced crystallization has been studied by means of birefringence measurements. The experiments were performed using an optical train consisting of a laser modulated by means of a rotating half-wave plate (OAM module, TA Instruments) and, at the other side of the shear cell, a circular analyzer and a photodetector. The intensity measured by the detector is given by

$$I \approx I_0[1 + \sin(4\Omega t + 2\varphi)\sin\delta] \quad (1)$$

with I_0 the initial intensity, Ω the angular velocity of the rotating half-wave plate, and φ the phase angle. The signal is analyzed using a decomposition of the form

$$I = I_{DC} + I_{sin}\sin(4\Omega t) + I_{cos}\cos(4\Omega t) \quad (2)$$

with I_{sin} and I_{cos} the amplitudes of the sine and cosine component in the signal.

The information contained in this signal is expressed in terms of the transmitted intensity I_{DC}, which is normalized with respect to the initial value of the intensity I_0 or $I_{DC}(t = 0)$ and of the birefringence $\Delta n'$:

$$\Delta n' = \frac{\lambda\delta'}{2\pi e} \quad (3)$$

with λ the laser light wavelength (670 nm), e the sample thickness, and δ' the optical retardation calculated as

$$|\sin \delta'| = \frac{\sqrt{I_{\sin}^2 + I_{\cos}^2}}{I_{DC}} \quad (4)$$

The optical train was combined with a sandwich-type shear cell, developed at the Solvay Central Laboratory.[28] In this setup, the sample is sheared between two parallel glass plates. The glass plates are incorporated in sample holders, which are placed in oppositely moving conditioning blocks. Apertures are provided in the equipment for laser light transition, allowing a view of the flow−vorticity plane of the sheared sample.

The setup allows achieving deformations up to a few hundred shear units, which is in the order of the shear rates realized in the outer layers of injection molded products. The unit is sufficiently rigid to withstand the normal forces generated during shear, even in case of highly viscous polymers.

The sliding plate concept ensures a constant shear rate throughout the sample. End effects can be minimized by a careful insertion of the sample between the glass plates. After crystallization, the sample thickness is typically between 50 and 100 μm.

More detailed information about the signal processing and the setup can be found in ref 28.

The isothermal crystallization protocol used in this study consists of an annealing step at 220 °C to erase the thermomechanical history of the material. Then, the sample is cooled to a chosen crystallization temperature of 145 °C at a rate of 5 °C/min.

The shearing protocol used consists of a shear step applied at the moment the crystallization temperature is reached (as proposed by the group of Janeschitz-Kriegl[6]). All shear steps are applied at a strain of ~100 units, and the shear rates vary between 20 and 420 s^{-1}.

The surface of the samples recuperated after the crystallization experiments was studied by means of light microscopy and atomic force microscopy (AFM) in order to determine the morphology. The microscope used was a Laborlux 12 Pol S, Leitz. The images of the microscope were registered by a digital camera (C4742-95, Hamamatsu Photonics) and saved by means of a frame grabber (HiPic 8.1.0, Hamamatsu Photonics). The AFM images were made using the True Non-Contact and Semi-Contact mode of a SmartSPM (AIST-NT).

3. Results and Discussion

Characterization of the Nucleating Ability and Quiescent Crystallization. In order to separate the contribution of particles and flow on the crystallization of the polymer, the nucleating ability of the various zinc oxide particles has to be assessed. Therefore, the zinc oxide mixtures were characterized by means of the Lotz efficiency scale for polymer nucleating agents,[50] which is an established protocol for characterizing the nucleating ability of particles mixed with a particular polymer. In view of the discussion in literature, the nucleating behavior of the particle is expected to be important in this study, and furthermore, the scale may provide a basis for comparison with other polymer−particle combinations.

The strength of the Lotz efficiency scale is that it references the nucleation in a filled polymer not only to a "lower limit", being the neat polymer, but also to an "upper limit". This upper limit is defined as the "ideally" nucleated polymer attainable by means of self-nucleation, creating nuclei which are "ideal" in terms of dispersion and chemical and crystallographic interactions. To create these, a nonisothermal DSC protocol is used. First the thermal history is erased in an annealing step (for polypropylene, at 210 °C). Then a standard crystallized state is created by cooling the polymer at a fixed rate of 10 °C/min to a temperature low enough to ensure full crystallization of the sample (for polypropylene, 50 °C is an adequate value). Next the crystallized polymer is partially melted in order to create stable crystal fragments. The concentration of these fragments saturates at a certain temperature. When nonisothermally cooled from this saturation temperature (for the polypropylene used in this study: 166 °C), the corresponding crystallization peak occurs at the highest temperature attainable by this procedure (for the polypropylene used in this study: 144 °C). This indicates the highest possible (ideal) nucleation of the polymer. Repeating the first two steps of this procedure for a filled polymer allows situating it with respect to the lower and upper nucleation limit.

Table 2. Nonisothermal Crystallization Peak Temperatures and Nucleating Efficiencies According to the Lotz Efficiency Scale for the Neat Polymer and the Different Polypropylene−1 wt % Zinc Oxide Mixtures

av diameter particles	(neat)	35 nm	200 nm	500 nm	1 μm
peak temp [°C]	116.0	118.4	117.2	117.7	121.3
NE [%]	0	8.7	4.3	6.3	21.7

Based on these experiments, the Lotz nucleating efficiency is defined as[50]

$$\mathrm{NE} = 100\frac{\Delta T_{NA}}{\Delta T} \quad (5)$$

with ΔT the difference between the nonisothermal crystallization peak temperatures of the neat (minimally nucleated) and the self-nucleated (maximally nucleated) polymer and ΔT_{NA} the difference between the nonisothermal crystallization peak temperatures of the neat polymer and the polymer with a certain percentage of the particles.

For the polymer−particle combination used in this study, the nucleating efficiencies are shown in Table 2.

The values in Table 2 are within the typical values of the NE, between 5% and 70%, except for the 200 nm zinc oxide, which is only just below 5% though. All values are at the lower end of the range, which agrees with the fact that uncoated zinc oxide is not commercially used as a nucleating agent for polypropylene.

Based on the specific surface data in Table 1, which is indicative of the contact surface between particle and polymer, it would be expected that the smallest particles have a larger nucleating ability. This would be the case if all particle characteristics except diameter were equal for the zinc oxides. However, as can be seen in Table 2, the nucleating efficiencies of the zinc oxide particles do not follow this reasoning. The observed deviations are probably caused by differences in the particle properties (shape, surface irregularities, slight differences in chemical composition, etc.).

It has to be remarked that for the mixtures with the 35, 200, and 500 nm zinc oxide the peak temperatures from the nonisothermal crystallization experiments are very similar, and the differences between them may even be considered to be within the expected experimental error. However, the question remains how the (differences in) nucleating ability will translate in terms of influence on the quiescent isothermal crystallization kinetics. This is measured by means of DSC at the crystallization temperature of 145 °C (see Figure 1). From this figure, it can be seen that all particle-filled polymers crystallize faster than the neat polymer, as is expected from their nucleating efficiency. These data show that the differences in nucleation as reported in Table 2, insignificant for three of the mixtures in nonisothermal crystallization experiments, are preserved and enlarged

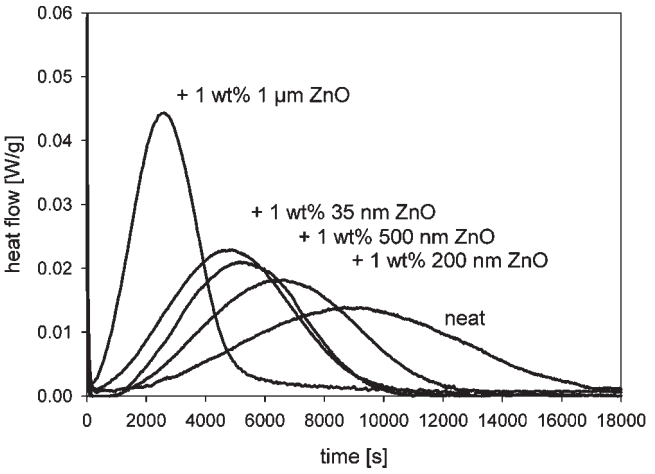

Figure 1. DSC heat flow vs time during isothermal crystallization at 145 °C for the different polypropylene−zinc oxide mixtures.

in the isothermal crystallization experiments. The crystallization kinetics of the neat polymer and the mixture with the 1 μm zinc oxide remain the slowest and fastest, respectively. But moreover, it can be seen from Figure 1 that, under these conditions, the mixture with the 200 nm zinc oxide crystallizes significantly slower than the mixture with the 500 nm zinc oxide, which in turn is significantly slower than the mixture with the 35 nm zinc oxide. Rheometric quiescent crystallization experiments have also been conducted and yielded similar results. More details about this approach can be found in the Supporting Information.

Although the quiescent crystallization kinetics of all mixtures are sufficiently distinguishable, the behavior of the mixtures with the 35, 200, and 500 nm zinc oxide are still very similar. Therefore, in the remaining part of this paper the kinetics of the mixture with the 200 nm zinc oxide will not be considered anymore.

Flow-Induced Crystallization: Typical Curves and Characteristic Values. In this study, the flow-induced crystallization has been monitored by means of birefringence and transmitted intensity measurements. These yield information both on the kinetics of crystallization and on the development of orientation during crystallization. In this work, the focus is mainly on the crystallization kinetics. In Figure 2, typical results for the neat polymer are shown.

Flow causes the isotropic conformation of the polymer molecules to be deformed, giving rise to birefringence.[51] The birefringence evolution during the shear step is usually referred to as flow birefringence (see Figure 2 (top)). For the lowest shear rates, it can be seen that the flow birefringence goes to a constant level and relaxes entirely to zero when the shear step is finished.

From a certain shear rate on (e.g., the curve at a shear rate of 255 s^{-1} in Figure 2 (top)), the flow birefringence does not relax entirely anymore when shear is stopped. This means that a significant measure of orientation remains present after the shear pulse. When the shear rate is increased even further, the flow birefringence exhibits an upturn at the end of the shear step (in Figure 2a, the curve at a shear rate of 255 s^{-1}), after which the birefringence signal only relaxes slightly before starting its crystallization-related increase. At the higher shear rates, the birefringence also exhibits a slight overshoot at the start-up of the shear. This phenomenon has been related to the stretching of polymer chains in the melt, causing overshoots in first and third normal stress differences (in respectively the flow−flow gradient plane and the flow−vorticity plane).[27]

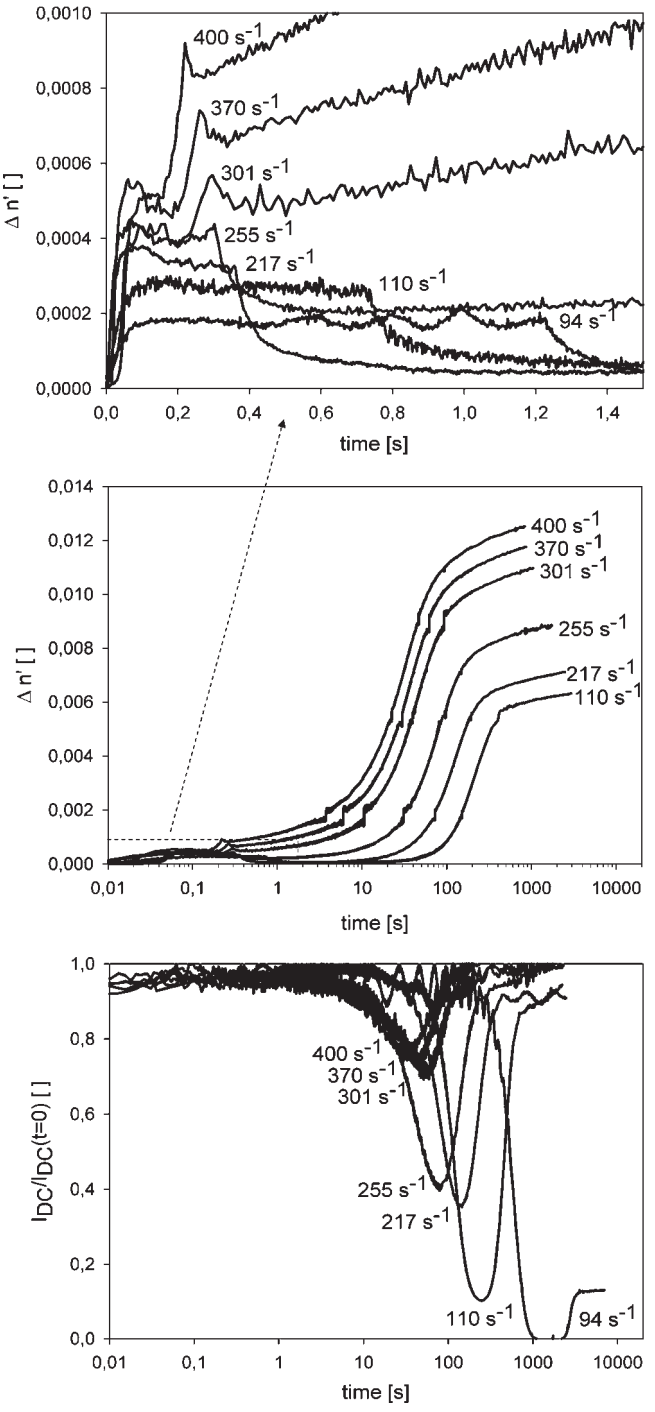

Figure 2. Development of birefringence $\Delta n'$ (top) during shear step, (middle), after shear step and (bottom) of normalized intensity $I_{DC}/I_{DC}(t = 0)$ during crystallization of neat polypropylene at 145 °C for different shear rates (strain ~100 units).

This evolution of the flow birefringence as a function of shear has also been observed by Kumaraswamy et al.[4,12,52] and Seki et al.[53] during their extrusion die experiments (constant wall shear stress, varying shear time) and by Langouche[28] and Baert et al.[29,54] in experiments with the same shear cell used in this study (constant strain, varying shear rate). Kumaraswamy et al.[4,12] proved by means of WAXD experiments that this upturn followed by incomplete relaxation indicates the presence of long-lived oriented structures, which form the template for subsequent strongly oriented crystal growth, more in particular, for shish-kebab structures.

The birefringence development during crystallization after the shear step exhibits a sigmoid shape (see Figure 2 (middle)). As the shear rate increases, the birefringence signal starts its increase earlier and its final plateau is at a higher level. In other words, the crystallization process accelerates and a higher level of orientation is reached in the sample, as was also observed by other authors.[28,29,48]

Furthermore, it can be seen that as the shear rate increases, relatively more time is needed for the birefringence signal to reach its final plateau. After its sharp sigmoid increase, it keeps increasing slowly toward a plateau level. This behavior was also seen during previous experiments with the shear cell. It indicates a more pronounced secondary crystallization mechanism for highly oriented samples. In the case of the strongly anisotropic (primary) crystalline structure encountered here, the secondary crystallization improves the existing lamellae or adds lamellae through an insertion mechanism, thereby contributing to the anisotropy.[28,29]

Additionally, the intensity evolution during crystallization is monitored (see Figure 2 (bottom)). Initially, as long as the sample is in a state of undercooled melt, the intensity remains constant. No significant change in the intensity level is observed during the shear step. Only when crystalline structures sufficiently large to scatter the laser light appear in the melt, the transmitted intensity decreases. For the lowest shear rates, the intensity goes to zero and remains at that value. For higher shear rates though, the intensity increases again after a certain time, causing a minimum to occur in the curve. Again, this observation is in accordance with observations for iPP by Langouche[28] and for PB by Baert et al.[29] Ding et al.[55] attributed the occurrence of this minimum to a loss of optical contrast between crystalline structure and melt due to impingement of the growing crystallites. With increasing shear rate, the minimum occurs faster and is less deep. This can be explained by the closer spacing of the growing spherulites and, at higher shear rates, the shish-kebabs. TEM images of fully shish-kebab dominated regions by Kumaraswamy et al.[12,13] show that for isotactic polypropylene the spacing of the shish typically goes from lengths close to the laser light wavelength (about 750 nm) to about 250 nm and possibly lower for higher shear rates. The kebab lamellae are too closely stacked to significantly scatter light.

In order to quantify the effect of shear rate at constant strain on the crystallization kinetics, characteristic times can be defined. Hereto, the time to the inflection point of the birefringence curve (termed "half time") and the position of the minimum in the intensity curve are chosen as characteristic times. Similarly, characteristic values could be defined for the level of orientation reached in the sample, but this issue is not addressed in this paper.

The shear rate dependence of the characteristics times is depicted in Figure 3 for the neat polymer. From this figure, it can be seen that both definitions yield similar results (see also refs 28, 29, and 52). The inflection point of the birefringence curve, to which the half time corresponds, indicates a change in the crystal growth rate, while the minimum of the intensity curve, as mentioned earlier, can be related to the impingement of the crystallites. Since impingement of the crystallites will change their growth speeds, this could explain the agreement between both characteristic times.[29]

At the lower shear rates, crystallization accelerates with increasing shear rate, followed, at the higher shear rates, by another acceleration. The data suggest that between these two acceleration regimes a transition region in the form of a plateau is present. Such a plateau, or saturation, has also been observed by Kumaraswamy et al.[52] (for constant wall shear stress and varying shearing time) and by Somani et al.,[26] by Vleeshouwer et al.,[20] and by Housmans et al.[24] (for constant strain and varying shear rate). However, in all these studies except the last one, the second acceleration was absent. Other authors, e.g., Vega et al.,[23] observe two regimes of acceleration, but without an intermediate regime. In the previous work with the sandwich-type shear cell,[28,29] the two regimes of acceleration are clearly discernible, while the presence of a plateau is arguable. In all studies though, the transition region, taking the form of a plateau or not, was shown to be connected to a change in morphology from spherulite-dominated to shish-kebab-dominated (in this study, through the appearance of an upturn in the flow birefringence). However, the precise mechanism behind this transition and its influence on the crystallization kinetics remain to be clarified.

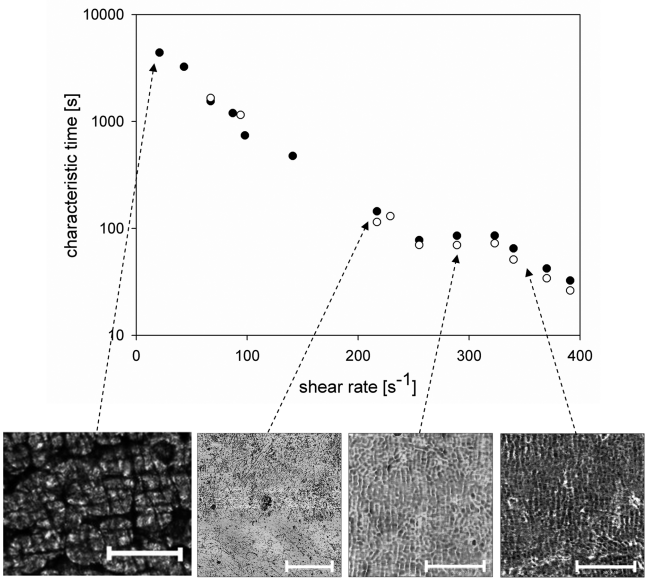

Figure 3. Dependence of characteristic values for kinetics (time to minimum of intensity: open symbols; half time from birefringence: filled symbols) on shear rate at a strain of ~100 units for neat polymer with below from left to right: microscopy image (reference line 100 μm), AFM phase images of neat polymer sample surface (flow direction horizontal, reference line respectively 1 μm, 300 nm, and 300 nm).

Flow-Induced Crystallization: Combined Effect of Particles and Flow. The approach explained in the previous section can also be applied to the polypropylene−zinc oxide mixtures. Figure 4 illustrates the effect of shear rate on the crystallization of a polypropylene mixed with 1 wt % 500 nm zinc oxide particles. As can be seen in this figure, the birefringence and transmitted intensity curves qualitatively have the same shape as the curves for the unfilled polymer, both during flow as during crystallization. The slopes corresponding to the increase of the birefringence signal (see Figure 4 (middle)), which can be associated with the growth rate of the crystallites,[13,29] are quantitatively similar to the slopes of the unfilled polymer (see Figure 2 (middle)). Hence, it can be concluded from these experiments that the particles do not significantly influence the growth speed during flow-induced crystallization. This is in agreement with the findings in the literature for quiescent conditions and with the observations by Kumaraswamy et al.,[4,13] who found that crystal growth after shear occurs at the same velocity as under quiescent conditions.

It can be seen that, from a certain shear rate on, the level of intensity transmitted through the fully crystallized sample is higher than the level of intensity transmitted through the melt (see Figure 4 (bottom)). This effect is more pronounced when the dimensions of the particles are closer to the wavelength of the laser light (632.8 nm). These particles scatter the laser light strongly when in the molten polymer, leading to an absolute

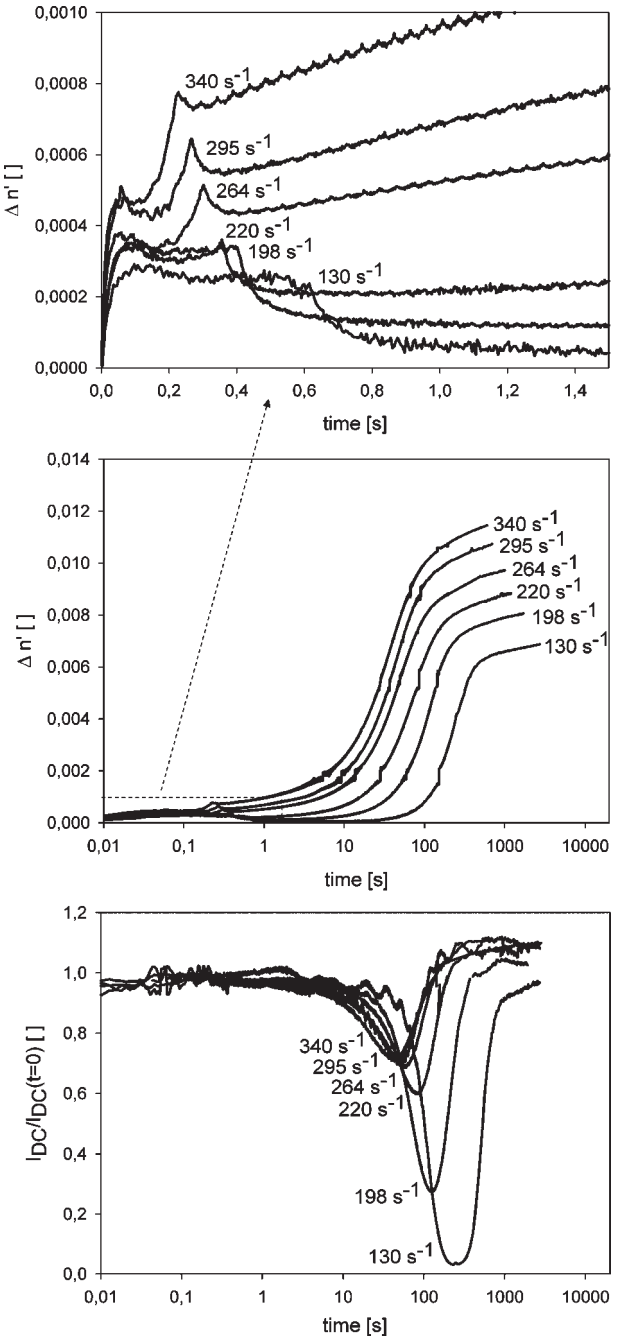

Figure 4. Development of birefringence $\Delta n'$ (top) during shear step, (middle) after shear step, and (bottom) of normalized intensity $I_{DC}/I_{DC}(t = 0)$ during crystallization of polypropylene with 1 wt % 500 nm ZnO at 145 °C for different shear rates (strain ~100 units).

intensity that is much less than for the unfilled polymer melt (e.g., for the polypropylene with 1 wt % 500 nm zinc oxide, the absolute intensity is 40% less). When these particles are embedded in a (sufficiently fine) crystalline structure, though, it appears that they scatter somewhat less than when in the melt, leading to an increased transmitted intensity at the end of the crystallization (e.g., for the polypropylene with 1 wt % 500 nm ZnO: normalized intensity transmitted through fully crystallized sample is about 10% more than for the molten sample at the highest shear rates). From these data, it might be hypothesized, in analogy with the theory proposed by Ding et al.,[55] that the encapsulation of the particles by a highly oriented crystalline structure causes a slight decrease in the optical contrast between the particle and the polymer.

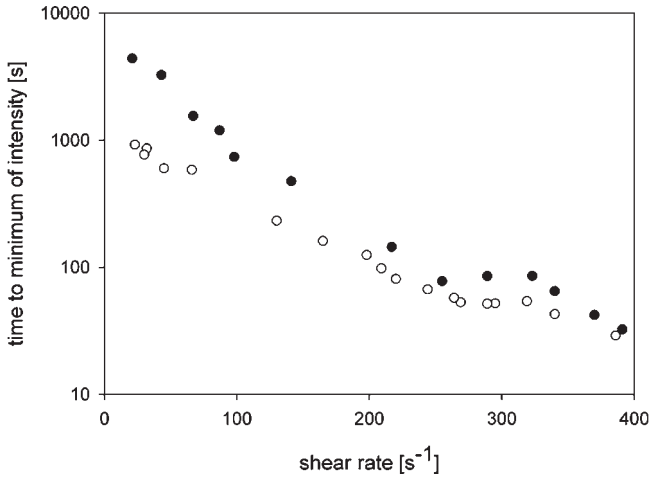

Figure 5. Dependence of time to minimum of intensity on shear rate at a strain of ~100 units for neat polymer (filled symbols) and mixture with 1 wt % 500 nm zinc oxide (open symbols).

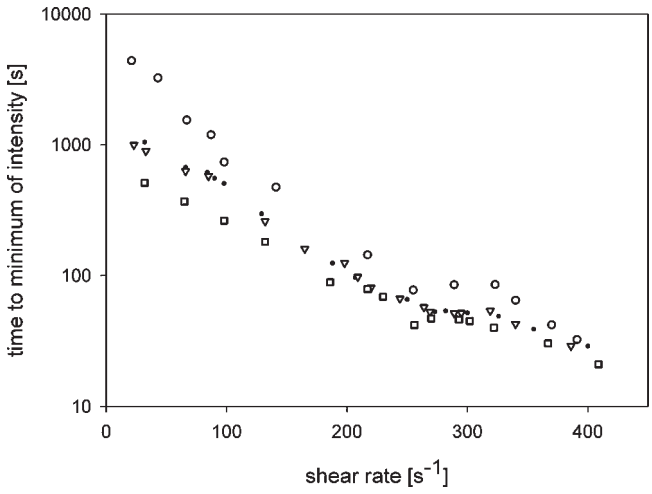

Figure 6. Dependence of time to minimum of intensity on shear rate at a strain of ~100 units for neat polypropylene (circles) and for polypropylene with 1 wt % 35 nm zinc oxide (dots), with 1 wt % 500 nm zinc oxide (downward triangles) and with 1 wt % 1 μm zinc oxide (squares).

In Figure 5, the characteristic crystallization times of the unfilled polypropylene and the polypropylene filled with 1 wt % 500 nm zinc oxide particles are compared. It can be seen that for the mixture the same regimes are present as for the neat polymer: there is an acceleration of the crystallization process at low to moderate shear rates and another one at high shear rates, while the data again suggest a transitional plateau. In the first regime, at relatively moderate shear rates, the slope of the curve for the mixture is less steep than for the neat polymer.

A comparison of the characteristic crystallization times for the polymer filled with 1 wt % of zinc oxide with different diameters is given in Figure 6. From this graph, it is clear that the difference in crystallization kinetics seen under quiescent conditions is still present at the lowest shear rates. At these shear rates, the neat polymer crystallizes the slowest and the mixture containing 1 wt % of the 1 μm zinc oxide the fastest. The mixtures with 1 wt % of the 35 nm zinc oxide and the 500 nm zinc oxide are in between. This is in agreement with the DSC and rheology data of crystallization under quiescent conditions reported before. Clearly, in the low shear region, the contribution of the particles to the

Table 3. Shear Rate at Which the Upturn in Flow Birefringence Is First Observed for Each Polypropylene−1 wt % Zinc Oxide Mixture

av diameter particles	(neat)	35 nm	500 nm	1 μm
$\dot{\gamma}_{upturn}$ [s^{-1}]	255	207	209	191

nucleation density overshadows the addition of nuclei caused by flow for the mixtures.

As Figure 6 shows that the difference between the characteristic values for the neat polymer and the different mixtures diminishes with increasing shear rate, it is clear that the competition between the particle and flow contributions to the nucleation density is a central issue. For the low to moderate shear rate region, the change in crystallization times is the largest for the unfilled material and the smallest for the mixture with the most powerful nucleating agent, i.e., the 1 μm particles. In other words, for these shear rates the effect of shear flow is less drastic for the materials with a higher nucleation density. As the unfilled polymer has the least nuclei in the quiescent case, the addition in terms of nuclei made by flow is relatively more important than for the mixtures, which have a larger nucleation density in the quiescent situation. This behavior corresponds with previous observations.[42−44,46−48]

As could be expected from the small difference in nucleation density reported earlier, and from the overall decrease in difference between the different materials as the shear rate is increased, no significant difference between the crystallization behavior of the mixtures with 35 and 500 nm zinc oxide can be seen anymore in this shear rate range.

At higher shear rates, in the transition region, the differences in characteristic times have become smaller than at the low shear rates, but the difference between the unfilled polymer and the mixtures is still very clear (see Figure 6). From this graph, the location of the transition is not unambiguous for each mixture. The shear rate at which the upturn in the flow birefringence appears first is a more marked parameter and therefore a better basis for comparison between the mixtures in this shear rate range. These shear rates are given for each mixture in Table 3.

The values in Table 3 show a systematic link between the nucleation density under quiescent conditions and the shear rate at which oriented precursors appear. The larger the nucleation density, the lower the shear rate at which the transition to shear-induced crystalline structures appear, although the effect is not very strong.

These results agree with previous observations that oriented structures appear at lower shear rates for particle containing polymers.[1,39,40,43,45−48] For the mixtures studied in this paper, the effect is not very strong, while in some studies concerning duct flow,[46] fiber-drawing experiments,[47,48] or injection molding[1] a more powerful effect was reported. In these, there is a complex and intense mechanical and thermal history, leading to a skin-core morphology, which may well magnify effects. The orientation enhancement during crystallization of intercalated montmorillonite clay mixtures was also reported to be very marked.[39,43,45] In these mixtures, there is a very small "interparticle" distance due to the specific nature of the particles, which may, according to the simulations by Hwang et al.,[49] be a key parameter to a significant synergy (stress amplification) between the polymer and matrix. The question remains though if the earlier occurrence of orientation is due to a synergetic effect or to the fact that the nucleation density at that shear rate is still higher for the polymer−particle mixtures, or if both influences are present, how they relate to each other.

At the highest shear rates used in this work, the measurements reported in Figure 6 show that the characteristic

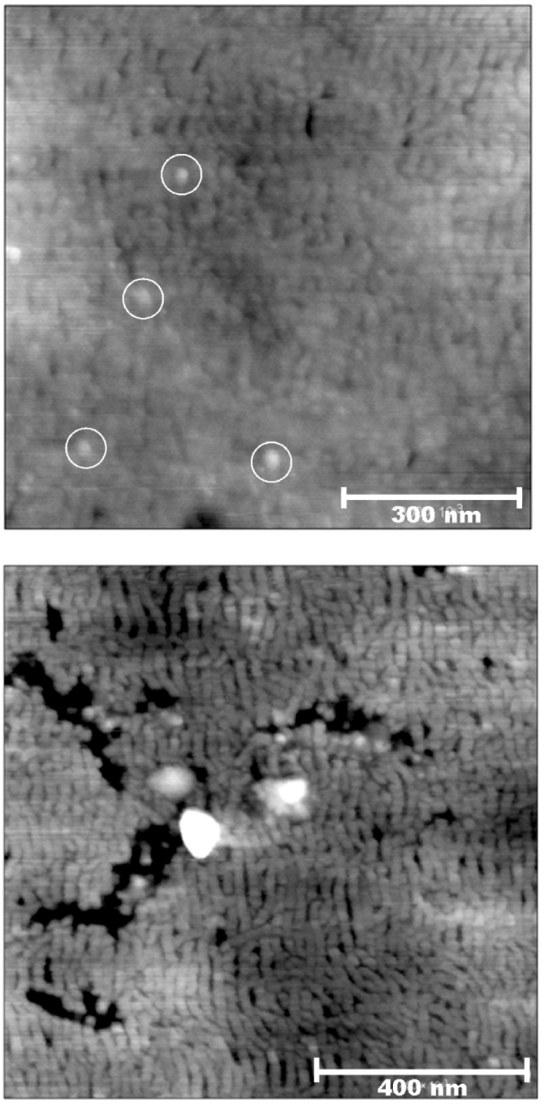

Figure 7. AFM height images of surface of (top) polymer with 35 nm ZnO (some particles are circled as an example) and (bottom) polymer with 200 nm ZnO (flow direction horizontal, reference line 300 and 400 nm).

crystallization times of the filled and unfilled polymer become very similar. The data suggest that, independent of the nucleating efficiency of the particles, flow dominates the kinetics of the crystallization process at these high shear rates.

Next to the effect of particles on the crystallization kinetics, the final morphology of the samples, recuperated from the experiments has been studied. Hereto, optical microscopy and AFM experiments have been performed. An example of such measurements for the unfilled polymer in shown in Figure 3.

At low shear rates, the morphology can still be observed by means of light microscopy, with e.g. at 20 s^{-1}, spherulites with a diameter of about 50 μm. As the shear rate increases, the nucleation density increases and, thus, the spherulitic structure becomes denser and finer. Toward the end of the first regime, the spherulites are too small to be discernible by light microscopy. AFM, on the other hand, allows visualizing them in the form of regions of lamellae, which are ordered in spherulites but because of the magnification appear in the images as oriented randomly.

Earlier in this paper, the appearance of an upturn in the flow birefringence has been pinpointed as indicative of

the transition from isotropic spherulitic crystals to oriented crystalline structures such as shish-kebabs. This can be verified by means of the AFM images. From the appearance of the upturn in the flow birefringence on and during the second acceleration, AFM shows the occurrence of structures oriented perpendicular to the flow direction. These are the kebabs; the lamellae nucleated on and growing radially from the shish. The extended polymer chains oriented in the flow direction which form the shish cannot be distinguished with this technique. The kebab lamellae can be seen to have a width of about 30−40 nm. They grow in length until they reach an obstacle or another lamella.

AFM can also be used to visualize how the particles are imbedded in the crystalline structure (see Figure 7). The 35 nm particles (Figure 7 (top)) are of similar dimensions as the width of the kebab lamellae. The growing lamellae can be stopped if the particle is directly in the path of the lamella; otherwise, the lamella continues around the particle, mostly retaining its orientation perpendicular to the flow. The other particle sizes used in this study form much larger obstacles. Kebab lamellae that come upon them are stopped or have to change direction to fill up the open space around the particle, e.g., 200 nm particles (Figure 7 (bottom)). In the literature, it has been suggested that occlusion or rejection of particles may disturb crystal growth,[38] though this was generally not found to be a very strong effect. Earlier it was shown that there is a quantitative agreement between the slopes of the birefringence curves for the neat polymer and its mixtures and, thus, between their crystal growth rates. The presence of the zinc oxide particles therefore does not seem to have a significant effect on the crystal growth rate in this study.

The effect on the shish formation though remains to be clarified.

4. Conclusions

In this paper, the influence of well-controlled simple shear, from low to processing rates, on the crystallization behavior of polypropylene with micro- to nanosized particles is presented. First, the nucleating efficiency was determined for the different zinc oxide particles using the Lotz efficiency scale. These results were mirrored in the quiescent crystallization kinetics. The shear-induced crystallization was monitored in birefringence experiments. Characteristic values were used to visualize the dependence of the kinetics on shear rate (at constant strain). From low to moderate shear rates, the crystallization accelerates with increasing shear rate. At the highest shear rates, a second acceleration of the crystallization process is observed. In the transition region between these accelerations, a plateau seems present, for which the characteristic crystallization times are relatively independent of shear rate. After a discussion of the neat polymer kinetics behavior, a comparison was made with the filled polymers. In the low shear rate region the differences between the neat polymer and the different mixtures with zinc oxide are most pronounced. The difference diminishes steadily with increasing shear rate. The occurrence of oriented structures takes place at a somewhat lower shear rate as the nucleating efficiency of the particle is higher. Therefore, nucleating efficiency, rather than particle diameter, dictates the behavior of the mixtures in this shear rate range. In the high shear rate region, there is no longer an influence of the presence of the particles; the crystallization kinetics is dominated by the intense shear flow, independent of the nucleating efficiency of the particles. Though the measurements do not exclude the existence of a synergetic interaction between particles and matrix, the (additive) competition between the particle and shear contribution to nucleation seems the determining factor of the behavior observed for these materials.

Acknowledgment. The authors thank Borealis GMBH and Umicore Group for providing the materials used in this study and Solvay for allowing the use of their facilities at Solvay Central Laboratory.

Supporting Information Available: Images of the different zinc oxides used in the study and rheology: characterization of the polypropylene and its mixtures with zinc oxide and quiescent crystallization. This material is available free of charge via the Internet at http://pubs.acs.org.

References and Notes

(1) Gahleitner, M.; Wolfschwenger, J.; Fiebig, J.; Neissl, W. *Macromol. Symp.* **2002**, *185*, 77–87.
(2) Housmans, J. W.; Gahleitner, M.; Peters, G. W. M.; Meijer, H. E. H. *Polymer* **2009**, *50* (10), 2304–2319.
(3) Kumaraswamy, G. *J. Macromol. Sci., Polym. Rev.* **2005**, *C45* (4), 375–397.
(4) Kornfield, J. A.; Kumaraswamy, G.; Issaian, A. M. *Ind. Eng. Chem. Res.* **2002**, *41* (25), 6383–6392.
(5) Janeschitz-Kriegl, H.; Eder, G. *J. Macromol. Sci., Part B: Phys.* **2007**, *46* (3), 591–601.
(6) Liedauer, S.; Eder, G.; Janeschitz-Kriegl, H.; Jerschow, P.; Geymayer, W.; Ingolic, E. *Int. Polym. Process.* **1993**, *8* (3), 236–244.
(7) Janeschitz-Kriegl, H.; Ratajski, E.; Stadlbauer, M. *Rheol. Acta* **2003**, *42* (4), 355–364.
(8) Pogodina, N. V.; Lavrenko, V. P.; Srinivas, S.; Winter, H. H. *Polymer* **2001**, *42* (21), 9031–9043.
(9) Koscher, E.; Fulchiron, R. *Polymer* **2002**, *43* (25), 6931–6942.
(10) Nobile, M. R.; Bove, L.; Somma, E.; Kruszelnicka, I.; Sterzynski, T. *Polym. Eng. Sci.* **2005**, *45* (2), 153–162.
(11) Liedauer, S.; Eder, G.; Janeschitz-Kriegl, H. *Int. Polym. Process.* **1995**, *10* (3), 243–250.
(12) Kumaraswamy, G.; Verma, R. K.; Issaian, A. M.; Wang, P.; Kornfield, J. A.; Yeh, F.; Hsiao, B. S.; Olley, R. H. *Polymer* **2000**, *41* (25), 8931–8940.
(13) Kumaraswamy, G.; Verma, R. K.; Kornfield, J. A.; Yeh, F. J.; Hsiao, B. S. *Macromolecules* **2004**, *37* (24), 9005–9017.
(14) van Meerveld, J.; Peters, G. W. M.; Hutter, M. *Rheol. Acta* **2004**, *44* (2), 119–134.
(15) Mykhaylyk, O. O.; Chambon, P.; Graham, R. S.; Fairclough, J. P. A.; Olmsted, P. D.; Ryan, A. J. *Macromolecules* **2008**, *41* (6), 1901–1904.
(16) Baert, J.; Van Puyvelde, P. *Macromol. Mater. Eng.* **2008**, *293* (4), 255–273.
(17) Kimata, S.; Sakurai, T.; Nozue, Y.; Kasahara, T.; Yamaguchi, N.; Karino, T.; Shibayama, M.; Kornfield, J. A. *Science* **2007**, *316* (5827), 1014–1017.
(18) Balzano, L.; Kukalyekar, N.; Rastogi, S.; Peters, G. W. M.; Chadwick, J. C. *Phys. Rev. Lett.* **2008**, *100* (4), 4.
(19) Baert, J.; Langouche, F.; Van Puyvelde, P. *Int. J. Mater. Form.* **2008**, *1*, 667–670.
(20) Vleeshouwers, S.; Meijer, H. E. H. *Rheol. Acta* **1996**, *35* (5), 391–399.
(21) Acierno, S.; Palomba, B.; Winter, H. H.; Grizzuti, N. *Rheol. Acta* **2003**, *42* (3), 243–250.
(22) Acierno, S.; Coppola, S.; Grizzuti, N. *J. Rheol.* **2008**, *52* (2), 551–566.
(23) Vega, J. F.; Hristova, D. G.; Peters, G. W. M. *J. Therm. Anal. Calorim.* **2009**, accepted.
(24) Housmans, J. W.; Steenbakkers, R. J. A.; Roozemond, P. C.; Peters, G. W. M.; Meijer, H. E. H. *Macromolecules* **2009**, *42* (15), 5728–5740.
(25) Baert, J.; Van Puyvelde, P. *Polymer* **2006**, *47* (16), 5871–5879.
(26) Somani, R. H.; Hsiao, B. S.; Nogales, A.; Srinivas, S.; Tsou, A. H.; Sics, I.; Balta-Calleja, F. J.; Ezquerra, T. A. *Macromolecules* **2000**, *33* (25), 9385–9394.
(27) Kumaraswamy, G.; Verma, R. K.; Kornfield, J. A. *Rev. Sci. Instrum.* **1999**, *70* (4), 2097–2104.
(28) Langouche, F. *Macromolecules* **2006**, *39* (7), 2568–2573.

(29) Baert, J.; Van Puyvelde, P.; Langouche, F. *Macromolecules* **2006**, *39* (26), 9215–9222.
(30) Pukanszky, B.; Moczo, J. *Macromol. Symp.* **2004**, *214*, 115–134.
(31) Vesely, D.; Ronca, G. *J. Microsc.* (*Oxford, U. K.*) **2001**, *201*, 137–143.
(32) Rybnikar, F. *J. Appl. Polym. Sci.* **1991**, *42* (10), 2727–2737.
(33) Pukanszky, B. *Eur. Polym. J.* **2005**, *41* (4), 645–662.
(34) Avella, M.; Cosco, S.; Di Lorenzo, M. L.; Di Pace, E.; Errico, M. E.; Gentile, G. *Eur. Polym. J.* **2006**, *42* (7), 1548–1557.
(35) Ferrage, E.; Martin, F.; Boudet, A.; Petit, S.; Fourty, G.; Jouffret, F.; Micoud, P.; De Parseval, P.; Salvi, S.; Bourgerette, C.; Ferret, J.; Saint-Gerard, Y.; Buratto, S.; Fortune, J. P. *J. Mater. Sci.* **2002**, *37* (8), 1561–1573.
(36) Tang, J. G.; Wang, Y.; Liu, H. Y.; Belfiore, L. A. *Polymer* **2004**, *45* (7), 2081–2091.
(37) Yuan, Q. N.; Jiang, W.; An, L. J.; Li, R. K. Y. *J. Polym. Sci., Part B: Polym. Phys.* **2005**, *43* (3), 306–313.
(38) Di Lorenzo, M. L. *Prog. Polym. Sci.* **2003**, *28* (4), 663–689.
(39) Nowacki, R.; Monasse, B.; Piorkowska, E.; Galeski, A.; Haudin, J. M. *Polymer* **2004**, *45* (14), 4877–4892.
(40) Kelarakis, A.; Yoon, K.; Sics, I.; Somani, R. H.; Chen, X. M.; Hsiao, B. S.; Chu, B. *J. Macromol. Sci., Part B: Phys.* **2006**, *45* (2), 247–261.
(41) Byelov, D.; Panine, P.; Remerie, K.; Biemond, E.; Alfonso, G. C.; de Jeu, W. H. *Polymer* **2008**, *49* (13−14), 3076–3083.
(42) Lagasse, R. R.; Maxwell, B. *Polym. Eng. Sci.* **1976**, *16* (3), 189–199.
(43) Somwangthanaroj, A.; Lee, E. C.; Solomon, M. J. *Macromolecules* **2003**, *36* (7), 2333–2342.
(44) Naudy, S.; David, L.; Rochas, C.; Fulchiron, R. *Polymer* **2007**, *48* (11), 3273–3285.
(45) Rozanski, A.; Monasse, B.; Szkudlarek, E.; Pawlak, A.; Piorkowska, E.; Galeski, A.; Haudin, J. M. *Eur. Polym. J.* **2009**, *45* (1), 88–101.
(46) Jerschow, P.; Janeschitz-Kriegl, H. *Int. Polym. Process.* **1997**, *12* (1), 72–77.
(47) Lu, F. M.; Spruiell, J. E. *J. Appl. Polym. Sci.* **1993**, *49* (4), 623–631.
(48) Spruiell, J. E.; Lu, F. M.; Ding, Z.; Richeson, G. *J. Appl. Polym. Sci.* **1996**, *62* (11), 1965–1975.
(49) Hwang, W. R.; Peters, G. W. M.; Hulsen, M. A.; Meijer, H. E. H. *Macromolecules* **2006**, *39* (24), 8389–8398.
(50) Fillon, B.; Thierry, A.; Lotz, B.; Wittmann, J. C. *J. Therm. Anal. Calorim.* **1994**, *42*, 721–731.
(51) Janeschitz-Kriegl, H. *Polymer Melt Rheology and Flow Birefringence* **1983**, xv+524.
(52) Kumaraswamy, G.; Issaian, A. M.; Kornfield, J. A. *Macromolecules* **1999**, *32* (22), 7537–7547.
(53) Seki, M.; Thurman, D. W.; Oberhauser, J. P.; Kornfield, J. A. *Macromolecules* **2002**, *35* (7), 2583–2594.
(54) Baert, J.; Langouche, F.; Van Puyvelde, P. *Fibres Text. East. Eur.* **2008**, *16* (6), 73–76.
(55) Ding, Z. M.; Spruiell, J. E. *J. Polym. Sci., Part B: Polym. Phys.* **1996**, *34* (16), 2783–2804.